A Multi-Year Data Set of Cloud Properties Derived for CERES from *Aqua*, *Terra*, and TRMM

Patrick Minnis
NASA Langley Research Center
Hampton, VA USA
p.minnis@nasa.gov

Patrick W. Heck
CIMSS
University of Wisconsin-Madison
Madison, WI USA

Sunny Sun-Mack, Qing Z. Trepte, Yan Chen, Ricky R. Brown, Sharon Gibson
SAIC
Hampton, VA USA

Xiquan Dong, Baike Xi
Department of Meteorology
University of North Dakota
Grand Forks, ND USA

***Abstract*—The Clouds and Earth's Radiant Energy System (CERES) Project is producing a suite of cloud properties from high-resolution imagers on several satellites and matching them precisely with broadband radiance data to study the influence of clouds and radiation on climate. The cloud properties generally compare well with independent validation sources. Distinct differences are found between the CERES cloud properties and those derived with other algorithms from the same imager data. CERES products will be updated beginning in late 2006.**

Keywords-clouds; MODIS; radiation; Aqua; Terra

I. INTRODUCTION *(HEADING 1)*

Simultaneous measurement of the radiation and cloud fields on a global basis has long been recognized as a key component in understanding and modeling the interaction between clouds and radiation at the top of the atmosphere, at the surface, and within the atmosphere. The NASA Clouds and Earth's Radiant Energy System (CERES) Project [1] launched its first broadband shortwave and longwave scanner on the Tropical Rainfall Measuring Mission (TRMM) in late 1997. This was followed by pairs of CERES scanners on the *Terra* and *Aqua* satellites during late 1999 and early 2002. Together, these satellites should provide the most comprehensive global characterization of clouds and radiation to date. Although the TRMM scanner failed during late 1998, the *Terra* and *Aqua* scanners continue to operate successfully.

CERES was designed to fly with high-resolution imagers so that the cloud conditions could be evaluated for every CERES measurement. Cloud properties are essential for converting the CERES radiances to the shortwave and longwave fluxes needed to define the Earth radiation budget (ERB). They are also critical for understanding the impact of clouds on the ERB. The 5-channel, 2-km Visible Infrared Scanner (VIRS) on the TRMM and the 36-channel, 1-km Moderate Resolution Imaging Spectroradiometer (MODIS) on *Terra* and *Aqua* are used to determine the cloud properties for each CERES footprint. To minimize inter-satellite differences and aid the development of useful climate-scale measurements, it was necessary to ensure that each satellite imager is calibrated in a fashion consistent with the other imagers and that the algorithms applied to one imager are as similar as possible to those applied to the other imagers. Thus, a set of cloud detection and retrieval algorithms were was developed that could be applied to all three imagers utilizing as few channels as possible while producing stable and accurate cloud properties. This paper summarizes the results of applying those techniques to more than 5 years of *Terra* MODIS, 3 years of *Aqua* MODIS, and 4 years of TRMM VIRS data.

NASA Science Mission through the CERES Project *(sponsors)*

II. DATA

Although the TRMM VIRS continues to operate, only data from January 1998 - July 2001 have been analyzed to date. The VIRS 0.65, 1.64, 3.75, 11.0, and 12.0-μm bands are used in the cloud detection and retrievals. *Terra* MODIS began collecting data in late February 2000 and continues to operate satisfactorily. *Aqua* MODIS became operational in July 2002 and is also still working. To date, the CERES cloud analysis algorithms have been applied to *Terra* and *Aqua* Collection-4 MODIS data through July 2005. The 1-km MODIS data are sampled every other pixel and scan line to reduce processing time. The CERES-MODIS (CM) cloud analysis algorithms use the 0.65, 1.38, 1.64 (2.13), 3.8, 6.7, 8.5, 10.8, and 12.0 μm channels. The CERES scanners measure broadband shortwave, total, and infrared window (8-12 μm) radiances with a nadir footprint of ~20 km.

Auxiliary data include the CERES Meteorology, Ozone, and Aerosol (MOA) dataset which includes vertical profiles of temperature and humidity. The CERES MOA profiles are based on the European Center for Medium-range Weather Forecasting (ECMWF) reanalyses for VIRS and on the Global Modeling Assimilation Office GEOS 4.03 [2]. Clear-sky albedos measured from VIRS and MODIS 0.65 and 1.6-μm data [3,4] are used with angular directional models to estimate the clear-sky reflectance for a given scene. Surface emissivities

[5] are used in conjunction with the reanalysis skin temperatures to estimate the clear-sky infrared radiances. The MOA data are used in the clear-sky radiance calculations. Topographic, surface type, snow and sea ice databases are also used in the analyses.

III. METHODOLOGIES

The results reported here are for the *Terra* Edition 2B and *Aqua* Edition 1A algorithms, which include cloud detection and retrieval. Each imager pixel is first classified as clear or cloudy using updated versions of the CERES classification schemes that employ the 0.64 (visible), 1.6 or 2.1 (near infrared), 3.7 (solar infrared), 10.8 (infrared), and 12 (split window) μm radiances [6,7]. The 1.6-μm channel is used as the near-infrared data for VIRS and *Terra*, while the 2.1-μm channel is used for *Aqua* because of problems with the *Aqua* 1.6-μm channel. To detect cloudy pixels, the radiances are compared with the predicted clear-sky radiances in a series of cascading tests. The differences between the 1.6 and 2.1-μm reflectances for clear snow surfaces necessitated some adjustments to the cloud mask algorithms [8]. An improved polar cloud detection algorithm was instituted for *Aqua* Edition 1 resulting in some large discrepancies between *Terra* and *Aqua* in polar regions.

Effective droplet radius r_e or effective ice crystal diameter D_e, optical depth τ, ice or liquid water path *IWP/LWP,* cloud temperature T_c, height z_c, thickness, and cloud phase are derived from these same radiances using one of three different techniques. The visible infrared solar-infrared split-window technique (VISST), an updated version of the original 3-channel daytime method [9], is used during daytime, which is defined as the time when the solar zenith angle *SZA* is less than 82°. At other times of day, the solar-infrared infrared split-window technique (SIST) is used to determine all of the parameters. The SIST, an improved version of the original 3-channel nighttime method [9], only uses thermal and solar infrared data. Thus, its retrievals are valid only for optically thin clouds. When the SIST is used, default values are used for all parameters except phase, T_c, and z_c for clouds with $\tau < 8$. The third method, pioneered by [10], is designated the solar-infrared infrared near-infrared technique (SINT) and is only applied to MODIS data during the daytime for clouds over snow or ice backgrounds. The 2.13-μm channel on *Aqua* is used instead of the 1.6-μm channel in the SINT. Determination of the background surface as snow or ice can either come from the scene classification for adjacent clear pixels or from the snow and ice maps used in the CERES data stream [7]. All of the methods compute both ice and liquid water solutions that simultaneously determine T_c, τ, and particle size. Each method iteratively matches the observed radiances to TOA radiances calculated using emittance and reflectance parameterizations that account for atmospheric attenuation and surface reflectance and emission. The cloud reflectances and emittances are included in the parameterizations [11, 12] using updated lookup tables for each specific channel. The phase is selected based on the cloud temperatures, the availability of a solution, best consistency with a solution, and cloud altitude.

The pixel-level data are convolved with the individual broadband CERES radiative fluxes to obtain the Single Scanner Footprint (SSF) dataset (Fig.1). These SSF products include the cloud fraction and mean associated properties for up to two cloud layers. No cloud properties could be retrieved for ~6.7% of pixels classified as cloudy during the daytime. At night, only 1.4% of the cloudy pixels are inconsistent with the parameterizations. Most no-retrieval pixels occur in polar regions over snow-covered surfaces or over very bright deserts. In the former instance, the SINT is unable to find a match, probably because of uncertainties in the clear-sky reflectance fields. In the latter case, the pixels detected as clouds may actually be heavy concentrations of aerosols that are misclassified as clouds. Over most ocean and land areas outside the polar regions and Saharan Desert, the no-retrievals account for 1 - 2% of the total number of cloudy pixels. To account for the no-retrieval pixels, the SSF convolution assigns the mean cloud properties from cloudy pixels in the footprint with retrieved values to the no-retrieval pixels, if more than 1/9 of pixels in the footprint have valid cloud retrievals. Otherwise, only the valid cloudy pixels are used and the no-retrieval pixels are not considered as part of the total number of pixels in the footprint.

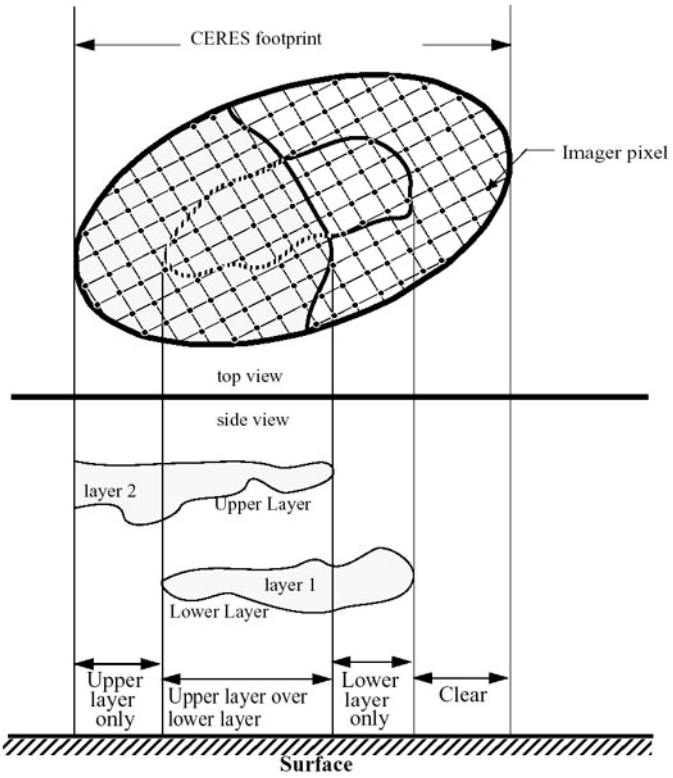

Figure 1. CERES SSF Clear/cloud layer/overlap illustration.

Imager pixel-level data are retained for data granules that include a selected number of locations around the globe for visual assessment and for comparison to independent validation datasets obtained from several research facilities around the world. Fig. 2 shows *Aqua* CM 30x30 km^2 average values of r_e, τ, and *LWP* compared with 1-hr means derived from radar and radiometer data at the Atmospheric Radiation Measurement (ARM) Southern Great Plains site using the methods of [13]. Means for each variable are given in the top panels followed by the standard deviations. Linear correlation coefficients are

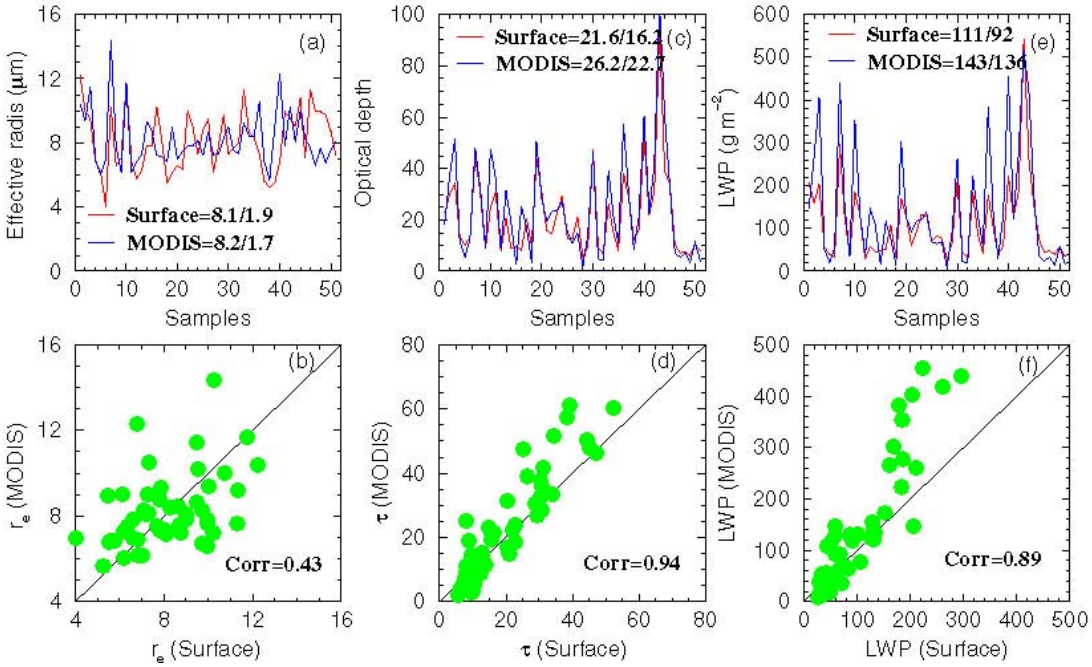

Figure 2. Comparison of stratus cloud properties from matched ARM SGP surface data and Aqua CERES-MODIS retrievals, July 2002-July 2004.

given in the bottom panels. The two datasets correspond closely except when τ is extremely large or small. For example, the value of r_e(CM) is significantly greater than its surface counterpart when $\tau < 10$. Many of the larger values of LWP(CM) exceed the surface values when LWP > 200 gm^{-2}. The results are typical for comparisons of surface-based LWP values with those from the CM method. Similar comparisons have been performed for cirrus clouds at the SGP and elsewhere [14, 15]. In general, the CM method does not detect clouds with $\tau < 0.3$.

IV. Results

Since examples of the results have been published elsewhere (e.g., [8,16]), some comparisons with another dataset are presented here. The MODIS Atmosphere Science Team (AST) is also generating cloud products from the same MODIS data as CERES, but using a different set of algorithms, models, and channels [17]. Fig. 3 shows the mean daytime cloud fractions from *Terra* for October 2003 from the CM analysis and the MOD08 Collection-4 average products from the MODIS AST. In most areas, the cloud amounts are very similar with differences less than ±10%. The CERES values are significantly larger over western Antarctica and portions of the Arctic, but are smaller than the MOD08 means in Mongolia, central and eastern Brazil, eastern Antarctica, portions of Greenland, and the warm pool of the Pacific. The corresponding daytime cloud-top pressures are plotted in Fig. 4, where the CM places cloud tops at greater pressures (lower heights) than MOD08 for most of the marine stratus areas and in the Arctic and Antarctic. The reverse situation occurs in most other regions. For example, the CM clouds at pressures less than 400 hPa cover a much larger area in the tropical warm pool than those from MOD08. The longitudinal gradients in the marine stratus cloud-top pressure are reversed. For example, the CM cloud pressures (heights) very gradually decrease (increase) from east to west by only 100 hPa from 80°W to 140°W at 15°S, while the MOD08 pressure rises by nearly 300 hPa. Mean cloud droplet effective radius for daytime data are plotted in Fig. 5. The patterns are very similar, but the CM values are smaller than the MOD08 values in nearly all areas, especially over the open ocean.

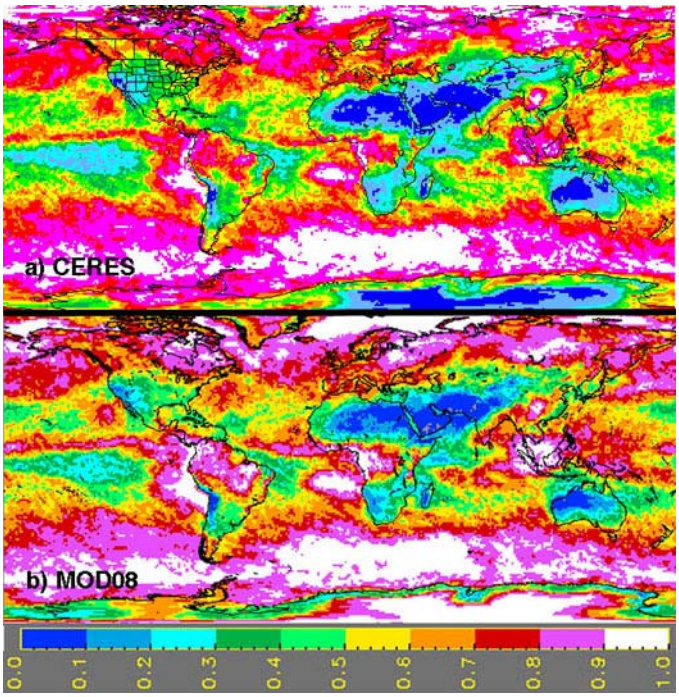

Figure 3. Mean daytime cloud amounts from Terra MODIS from (a) CM and (b) MODIS AST algorithms, October 2003.

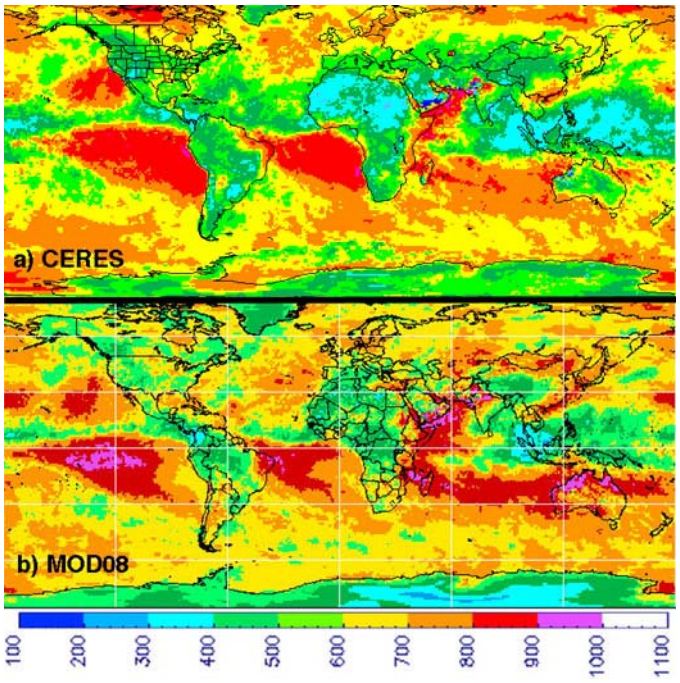

Figure 4. Same as Fig. 3, except for cloud-top pressure in hPa.

V. SUMMARY

The unique CERES cloud-radiation dataset now covers more than 5 years. Initial evaluations indicate that the cloud properties are of reasonable accuracy and will be useful for climate studies. Further validation and studies to understand the differences between the MODIS AST and CERES products are continuing. Because the MODIS data have been revised in the Collection-5 series, the CERES cloud products will be soon be reprocessed using Edition-3 algorithms, and analysis will continue for the life of the instruments.

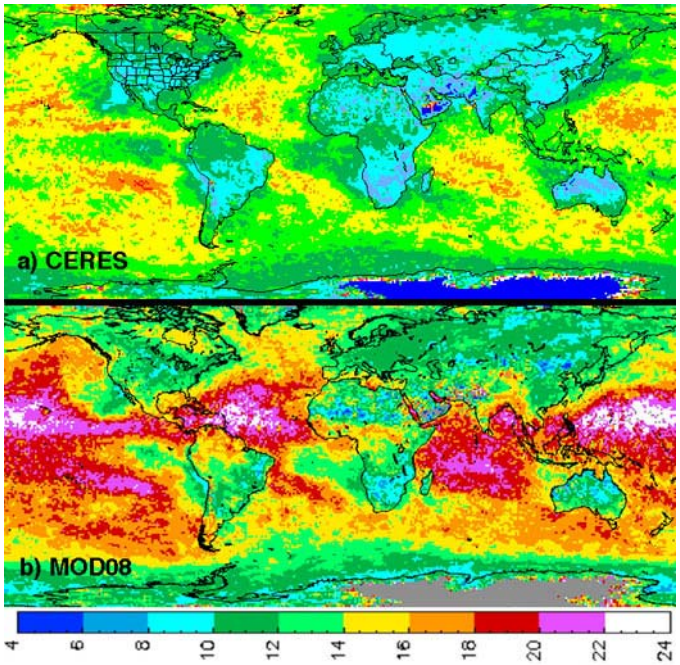

Figure 5. Same as Fig. 3, but for r_e (μm). Deep blue/gray areas = no liquid.

REFERENCES

[1] Wielicki, B. A., et al., "Clouds and the Earth's Radiant Energy System (CERES): Algorithm overview," IEEE Trans. Geosci. Remote Sens., vol. 36, pp. 1127-1141, 1998.

[2] DAO, "GEOS-3 Data Assimilation System Architectural Design," DAO Office Note 97-06. Data Assimilation Office, Goddard Space Flight Center, Greenbelt, MD 20771, 1997.

[3] Sun-Mack, S., Y. Chen, T. D. Murray, P. Minnis, and D. F. Young, "Visible clear-sky and near-infrared surface albedos derived from VIRS for CERES," Proc. AMS 10th Conf. Atmos. Rad., Madison, WI, June 28 – July 2, pp. 422-425, 1999.

[4] Sun-Mack, S., P. Minnis, Y. Chen, and R. F. Arduini, "Clear-sky narrowband albedos derived from VIRS and MODIS," Proc. SPIE 10th Intl. Symp Remote Sens., Conf. Remote Sens. Clouds and Atmos., Barcelona, Spain, September 8-12, pp. 101-109, 2003.

[5] Chen, Y., S. Sun-Mack, P. Minnis, D. F. Young, and W. L. Smith, Jr., "Surface spectral emissivity derived from MODIS data," Proc. SPIE 3rd Intl. Asia-Pacific Environ. Remote Sensing Symp, Hangzhou, China, October 23-27, vol. 4891, 361-369, 2002.

[6] Trepte, Q., Y. Chen, S. Sun-Mack, P. Minnis, D. F. Young, B. A. Baum, and P. W. Heck, "Scene identification for the CERES cloud analysis subsystem," Proc. AMS 10th Conf. Atmos. Rad., Madison, WI, June 28 – July 2, 169-172, 1999.

[7] Trepte, Q., P. Minnis, and R. F. Arduini, "Daytime and nighttime polar cloud and snow identification using MODIS data," Proc. SPIE 3rd Intl. Asia-Pacific Environ. Remote Sensing Symp. 2002, Hangzhou, China, October 23-27, vol. 4891, 449-459, 2002.

[8] Minnis, P., et al., "CERES cloud property retrievals from imagers on TRMM, Terra, and Aqua," Proc. SPIE 10th Intl. Symp Remote Sens., Conf. Remote Sens. Clouds and Atmos., Barcelona, Spain, Sept. 8-12, 37-48, 2003.

[9] Minnis, P., et al., 1995: "Clouds and the Earth's Radiant Energy System (CERES) Algorithm Theoretical Basis Document, Volume III: Cloud Analyses and Radiance Inversions (Subsystem 4)", NASA RP 1376 vol. 3, pp. 135-176, 1995.

[10] Platnick, S., J. Y. Li, M. D. King, H. Gerber, and P. V. Hobbs, "A solar reflectance method for retrieving cloud optical thickness and droplet size over snow and ice surfaces," J. Geophys. Res., vol. 106, 15185-15199, 2001.

[11] Minnis, P., D. P. Garber, D. F. Young, R. F. Arduini, and Y. Takano, "Parameterization of reflectance and effective emittance for satellite remote sensing of cloud properties," J. Atmos. Sci., vol. 55, 3313-3339, 1998.

[12] Arduini, R. F., P. Minnis, and D. F. Young, "Investigation of a visible reflectance parameterization for determining cloud properties in multi-layered clouds," Proc. 11th AMS Conf. Cloud Physics, Ogden, UT, June 3-7, CD-ROM, P2.4, 2002.

[13] Dong, X., P. Minnis, G. G. Mace, W. L. Smith, Jr., M. Poellot, R. T. Marchand, and A. D. Rapp, "Comparison of stratus cloud properties deduced from surface, GOES, and aircraft data during the March 2000 ARM Cloud IOP," J. Atmos. Sci., vol. 59, 3256-3284, 2002.

[14] Mace, G. G., Y. Zhang, S. Platnick, M. D. King, P. Minnis, and P. Yang, "Evaluation of cirrus cloud properties from MODIS radiances using cloud properties derived from ground-based data collected at the ARM SGP site," J. Appl. Meteorol., vol. 44, 221-240, 2005.

[15] Chiriaco, M., et al., "Comparison of CALIPSO-like, LaRC, and MODIS retrievals of ice cloud properties over SIRTA in France and Florida during CRYSTAL-FACE," In press, J. Appl. Meteorol. Climatol, 2006.

[16] Minnis, P., et al., "Diurnal, seasonal, and interannual variations of cloud properties derived for CERES from imager data," Proc. 13th AMS Conf. Satellite Oceanogr. & Meteorol., Norfolk, VA, Sept. 20-24, CD-ROM, P6.10, 2004.

[17] King, M. D., et al., "Cloud and aerosol properties , precipitable, water, and profiles of temperature and water vapor," IEEE Trans. Geosci. Remote Sens., vol. 41, 442-458.